Heliyon 9 (2023) e20939

Contents lists available at ScienceDirect

Heliyon

journal homepage: www.cell.com/heliyon

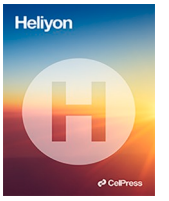

Thermal, morphology and bacterial analysis of pH-responsive sodium carboxyl methylcellulose/ fumaric acid/ acrylamide nanocomposite hydrogels: Synthesis and characterization

Shanmugavel Sudarsan [a,**], Evgeny Trofimov [a], D.S. Franklin [b], Selvam Mullai Venthan [c], Selvam Guhanathan [b], Sanjay Mavinkere Rangappa [d,*], Suchart Siengchin [d]

[a] South Ural State University, Chelyabinsk, 454080, Russia
[b] Department of Chemistry, Muthurangam Govt. Arts College (Autonomous), Vellore, 632002, Tamilnadu, India
[c] Department of Mathematics, Amrita School of Engineering, Amrita Vishwa Vidyapeetham, Bangaluru, India
[d] Natural Composites Research Group Lab. Department of Materials and Production Engineering, The Sirindhorn International Thai-German Graduate School of Engineering (TGGS), King Mongkut's University of Technology North Bangkok (KMUTNB), Bangkok, Thailand

ARTICLE INFO

Keywords:
Hydrogels
Fumaric acid
Carboxymethyl cellulose
Acrylamide
Nanocomposite
Swelling studies

ABSTRACT

In this present investigation, sodium carboxymethyl cellulose grafted with Fumaric acid/Acrylamide (CMC/FA/AAm=CFA) hydrogel and their silver nanocomposite hydrogels (CFA-Ag $_x$, x = 5, 10 and 20) were developed by simple, cost effective and ecofriendly greener method. Mint leaf extract was used as an efficient natural reducing agent due to presence of active and antioxidant potential of polyphenol and flavonoid components. Swelling equilibrium of CFA hydrogel showed S_{eq}% 3000 both in pH medium and distilled water. CFA (90:10) hydrogel has been produced greater than S_{eq}% 6000. The synthesized CFA (90:10)-Ag-5, CFA (90:10)-Ag-10 and CFA (90:10)-Ag-20 nanocomposite hydrogels have been observed lower S_{eq}% 2000–3000 than the CFA hydrogel. The homogeneous distribution of AgNPs throughout the CFA hydrogel and nanocomposites has been explored by SEM analysis. The interaction of network heteroatoms with AgNPs has been strongly revealed by the FTIR spectra and XRD analysis. The thermal stability of CFA (90:10)-Ag-5, 10, and 20 nanocomposite hydrogels have showed greater stability than CFA hydrogel which is confirmed by TGA/DSC thermogram analysis. The TEM analysis was used to explore a uniform distribution of spherical AgNPs (10 nm–50 nm) embedded on the CFA composite hydrogel. The CFA (90:10)-Ag-20 nanocomposite hydrogel has showed good antibacterial activity beside *E. coli* (Gram positive) and *S. aureus* (Gram negative) pathogens. Based on the antibacterial activity and swelling properties of CFA-Ag nanocomposite hydrogels have the ability to accelerate the antibacterial activity and are potential candidates for medical and environmental applications.

* Corresponding author.
** Corresponding author.
E-mail addresses: srsudarsan29@gmail.com (S. Sudarsan), mavinkere.r.s@op.kmutnb.ac.th (S. Mavinkere Rangappa).

https://doi.org/10.1016/j.heliyon.2023.e20939
Received 23 April 2023; Received in revised form 10 October 2023; Accepted 11 October 2023
Available online 27 October 2023

1. Introduction

Hydrophilic 3D hydrogel networks have expected considerable devotion in previous few decades due to their absorption of huge quantity of water and physiological body fluids and an exceptional premise in medical related applications. They have a strong similarity to existing tissues due to their relatively more water content and elastic consistency. Foremost advantage of this innovative biomaterial is its stability under varying pH, temperature and tonicity conditions [1,2]). Smart hydrogels have noticed sensational behaviour of variations in the environmental conditions like pH, light, magnetic and temperature which respond by altering the degree of swelling [3,4]. This sensing competence is being selected in numerous medical based applications viz., tissue engineering, drug delivery and soft wound materials etc [5,6]. The peculiar features of stimulus-responsive hydrogel stimuli have been found to have a lot of applications in the fields of biomedical and pharmaceutical such as artificial tendons and organs, soft contact lenses and self-regulated, pulsatile or oscillating drug delivery systems [7–11]. Furthermore, the development of chemical valves, immobilization of enzymes and cells, in bulk engineering for microfluidic devices, motors/actuators, sensors, tissue engineering material chromatography and micro-adhesion materials [12].

pH parameter is a vital environmental factor for organizations due to precise or pathological body locations, like intestine, blood vessels, stomach, vagina and tumor places, lysosomes and endosomes differ in pH values [13,14]. Anionic and cationic pH-responsive hydrogels has discussed from carboxylic acids like poly acrylic acid (PAA) and poly methacrylic acid (PMAA) [1], Citric acid and poly-glutamic acid (PLG) [1,15], itaconic acid [16], poly (2-dimethylamino ethyl methacrylate) (PDMAEMA), poly- (2-[vinyl pyridine]) (PVP) [17], acrylamide and chitosan hydrogels [5,18,19].

Sodium Carboxymethyl Cellulose (NaCMC) is the utmost plentiful and bio-recyclable source available on world [20–22]. The novel functional material consequent from cellulose has been used for a wider range of applications. Recently, biocompatible and environmentally friendly-based polymeric materials have been focused on. NaCMC related hydrogels shows numerous promising assets like biodegradability, hydrophilic nature, biocompatibility, cost effective and non-toxic [23–25]. The NaCMC is a type of polyelectrolyte which is known as "smart" cellulose imitative and it is responds to different pH and ionic medium solution. The formation of hydrogel is also very easy because of greater number of reactive hydroxyl groups present in polymeric chains [26,27]. Stimuli responsive hydrogels have been fabricated with the interaction of physical cross-linking of CMA and fumaric acid, which is because of presence of poly-hydroxyl groups, which can participate in hydrogen bonding [28,29]. Therefore, NaCMC is exact challenging to soften in usual solvents because of its greatly stretched structure of hydrogen-bond [30,31].

Fumaric acid (FA) is a bi-functional carboxylic acid with an unsaturated reactive site. FA can act as starting materials for polyesterification of polymeric hydrogels [30,32,33] and it has shown excellent biological activity. It is non-toxic, biocompatible, readily available and an inexpensive monomer. FA is widely utilized in medicine and food technology ([34,35]). Acrylamide (AAm) consists of a double bond and an amide group which is used to tune the smart responsive behaviour in hydrogels [36]). AAm hydrogels has shown a changeable swelling kinetics, which is applicable in release of insulin to increase osteoblast adhesion behaviour [37–41].

The addition of inorganic nano size particles within a three-dimensional polymeric hydrogel network as also discussed [42]. Nano level silver particles (AgNPS) have been extensively used in sodium alginate hydrogel [6], which is due to significant enhancement in performance properties viz., high swelling or deswelling rates, mechanical toughness, excellent electrical conductivity, large deformability, antimicrobial effects and optical properties [43]. The reduction of metal ions into hydrogel matrix has been noticed in many articles [44]. However, the synthesis route is harsh because of toxic nature of reducing agent. Many methods had done for the fabrication of nanocomposite hydrogels by several ways, such as chemical reduction, chemical vapour deposition and laser ablation etc. To overcome such drawbacks, researchers are interested in enhancing greener conditions using natural plant extract as a reducing agent due to simple technique, low cost, greener approach and ambient conditions for reduction reaction [14,45,46].

The novelty of present work, from the environmental concern, the synthesized method labeled is relatively simple, low cost and ecofriendly greener in situ synthesis technique was established where an active ingredient from mint leaf extract was involved with silver nanoparticles and carboxyl methylcellulose/fumaric acid/acrylamide (CFA) to form CFA-Ag nanocomposites. The synthesized CFA nanocomposite hydrogel is a better candidate for antibacterial activity beside *E. coli* (Gram positive) and *S. aureus* (Gram negative) pathogens and antimicrobial applications. The effect of CFA hydrogel and CFA-Ag nanocomposite hydrogels properties (swelling and pH sensitivity) was also discussed.

In this present investigation, which is based on the greener approach, methods were involved for synthesis of eco-friendly nanocomposite hydrogels using renewable resource monomers and polyol and mint extract. The pH-sensitive CFA hydrogels has been fabricated via radical polymerization of sodium carboxylmethyl cellulose, fumaric acid and acrylamide with the presence of N, N'-methylene bisacrylamide cross-linker and potassium persulphate initiator. The reduction of silver nitrate ($AgNO_3$) into AgNPs has been carried out using natural reducing agent like mint leaf extract with in the swollen hydrogel [47–50]. The developed CFA nanocomposite hydrogels were characterized by spectral, thermal and morphological observations such as FT-IR, TGA and SEM analysis. The imbibed Ag^+ ion inside the hydrogel has been explained by XRD and TEM analysis. Swelling equilibrium studies are also done and it leads to biomedical applications. The CFA nanocomposite hydrogels have exhibited excellent antibacterial activity against *E. coli* (Gram positive) and *S. aureus* (Gram negative) pathogens.

2. Experimental

2.1. Materials and methods

Research grade chemicals were used throughout the investigation. Carboxymethyl cellulose sodium salt (NaCMC) was procured

from SD Fine Chemical Limited, India. Fumaric acid (FA) was obtained from Merck Limited India. Acrylamide (AAm) was purchased from SRL Pvt. Ltd, Maharashtra, India. Potassium per sulphate (KPS), N, N'-Methylene bisacrylamide (MBA), Silver Nitrate ($AgNO_3$) was obtained from Avra Chemicals, India. Mint is collected from local shop in Ambur, Tamilnadu. Double distilled water was utilized for the polymerization reaction.

2.2. Synthesis of CFA hydrogels

An appropriate amount of NaCMC was liquefied in 50 ml distilled water. The 1 % of initiator of KPS was added with constant stirring for 1h. After 1h, a known amount of acrylamide and fumaric acid were added along with N, N'- Methylene bisacrylamide to the intermediate product then it is constantly stirred for 20 h at 70 °C. The achieved CFA hydrogels has been submerged in adequate distilled water in room temperature. The excess chemical soluble components were removed by the above method. The final swollen hydrogel has dried in vacuum hot oven to attain at constant weight. The chemical compositions of CFA based hydrogels has shown in Table 1.

2.3. Extraction of mint leaf

The standard procedure has been followed for mint leaf extract. The double distilled water (DW) was used for washed mint leaves. 2.5g of mint leaves has been immersed in 100 ml distilled water in 500 ml beaker and it was heated at 100 °C for 2 min. The obtained hot greenish colour solution cooled at room temperature then filtered through Whatman 40 filter paper. The resultant extract was stored at 4 °C for future use [6].

2.4. Synthesis of CFA-Ag nanocomposite hydrogel via green approach

A series of CFA hydrogels was permitted to swelling in DW to 3 h for reach swelling equilibrium. The CFA hydrogel exhibited superb swelling rate in DW. Nanocomposite hydrogels were prepared from the best swelling CFA (90:10) hydrogel. Three different concentrations of silver nitrate (AgNO3) solutions such as 5 mM, 10 mM, and 20 mM for the preparation of nanocomposite. The swollen hydrogels were immersed in 50 ml beaker, which contain 20 ml of $AgNO_3$ solution of different concentration for 6 h separately to reach equilibrium state. Maximum numbers Ag^+ ions has been entered into the hydrogel network during the equilibrium state. As a final point, the 20 ml of mint leaf extract has been utilized for the reduction of Ag^+ ion-loaded hydrogels at 6 h at room temperature. Huge amounts of Ag + ions have been reduced into Ag^0 which gives Ag-loaded nanoparticles. The blackish brown colour sample has confirmed the formation of CFA-Ag nanocomposite hydrogels and it was dried in vacuum oven, and then cooled at room temperature. The obtained product has rumpled well for additional characterization. Chemical composition of CFA-Ag nanocomposite hydrogels has shown in Table .2. The schematic representation of CFA-Ag nanocomposite hydrogel mechanism has been depicted in Scheme 1.

2.5. Swelling studies

The minimum quantity of known weight of hydrogel has been submerged in different swelling solution such as Distilled water and pH solutions for one day at normal room temperature. The swollen hydrogel has been weighed without excess water [11]. As per the equation the swelling ratio and equilibrium water content has been calculated,

$$S_{eq}\% = \frac{W_{eq}\text{-}W_d}{W_d} \times 100 \quad (1)$$

where, W_{eq}- Weight of swollen hydrogel at equilibrium and W_d-Weight of dry hydrogel.

2.6. FT-IR spectral studies

FTIR spectrophotometer was used for recorded FT-IR spectra (Shimadzu, 8400, Japan) in KBr pellet medium in the range of 400 and 4000 cm^{-1}.

Table 1
Chemical compositions of CFA based hydrogels.

Sample Index	CMC (g)	FA (g)	AAm (g)	MBA (g)	$K_2S_2O_8$ (g)
CFA	1	1	1	0.03	0.03
CFA (10:90)	0.10	0.90	1	0.02	0.02
CFA (30:70)	0.30	0.70	1	0.02	0.02
CFA (50:50)	0.50	0.50	1	0.02	0.02
CFA (70:30)	0.70	0.30	1	0.02	0.02
CFA (90:10)	0.90	0.10	1	0.02	0.02

Table 2
Feed compositions of CFA-Ag nanocomposite hydrogels.

Sample Index	Gel (g)	Mint extract (ml)	Ag NO_3 (mM)
CFA (90:10)-Ag-5	1	20	5
CFA (90:10)-Ag-10	1	20	10
CFA (90:10)-Ag-20	1	20	20

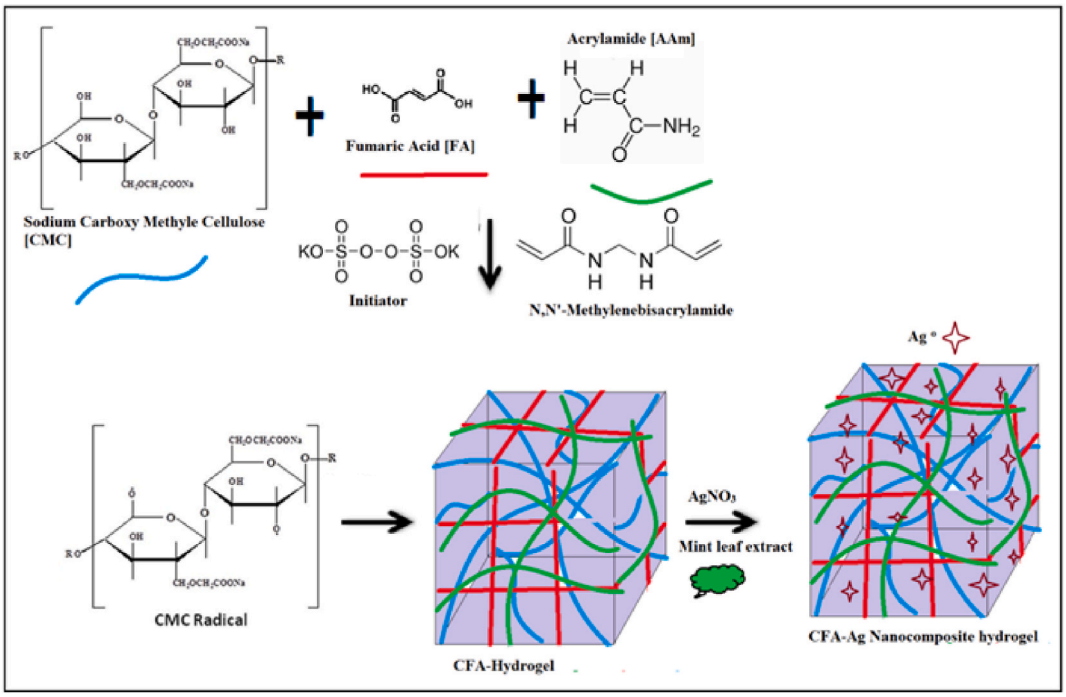

Scheme 1. The fabrication of CFA-Ag nanocomposite hydrogel.

2.7. X-ray diffraction (XRD) analysis

The crystalline-amorphous nature of plain and silver nanocomposite hydrogels were done by X-ray diffraction (XRD) analysis in BRUKER, Germany model named D8 Advance. The source of 2.2 KW Cu anodes, ceramic X-ray tube optimized. Cu radiation = 0.1546 nm) consecutively at 40 kV and 40 mA. The diffractogram was observed in from 10 to 70°at speed rate of 2°/min.

2.8. Thermogravimetric analysis (TGA)

The thermal analysis has been carried out by SDT Q600 TGA instrument (TA Instruments-Water LLC, Newcastle, DE) at a heating rate of under a continuous nitrogen flow (100 ml/min) and the materials were run from 40 to 800 °C.

2.9. Morphological analysis (SEM/TEM)

2.9.1. Scanning electron microscopy (SEM)

The surface photo of hydrogels and nanocomposite hydrogels was examined under SEM studies (SEM, JEOL JSM-5410LV). The samples were cut into small fragments; mounted onto aluminum stumps and sputter covered with gold at 10–20 nm thickness previous to the statement.

2.10. Transmission electron microscopy (TEM)

TEM was done on a JEOL JEM-2100. For this study, preparation of a sample by scattering two to three droplets (1 mg/ml) of excellently divided sample solution on a 3 mm copper grating and aeration at moderate temperature, which was worked at voltage of 120 kV.

2.11. Antibacterial assessment

The bacterial cultures were sub-cultured occasionally and preserved on nutrient agar (NA) average at room temperature (30 ± 2 °C) for additional investigates. The antibacterial activity has established changed with agar well diffusion method. Muller–Hinton agars were pasteurized, dispensed on Petri plates and permissible to solidify under laminar airflow. About 100 μl [108 CFU/ml (colony forming units)] of each bacterial culture was supper on the agar surface by a sterile glass spreader. Wells of 10 mm diameter were made utilized sterile corn borer on the agar medium. About 100 ml (0.025–0.25 mg) of samples were added to the well and they kept in the refrigerator for 20 min for diffusion. Then, the plates were incubated for 24 h at 37 °C and control as ethanol. The antibacterial activity was assessed by calculating the diameter of zone of inhibition against the test organisms.

3. Results and discussion

The NaCMC, FA and AAm were utilized for the synthesis of CFA hydrogels and their CFA-Ag nanocomposite hydrogels. The sulphate anion is produced from the thermally decomposition reaction of potassium per sulphate ($K_2S_2O_8$), which abstracts hydrogen from one functional group in the side chain (i.e. COOH, OH, SH and NH2) of the substrate to form corresponding radicals [51]. Sulphate anion forms radical hydrogen atoms to form the OH group of NaCMC to form the macromolecular substrate. MBA acts as a cross-linker and forms four reactive radical sites, which are used to form crosslinks between NaCMC and vinyl monomers. Later, the cross-linking three-dimensional polymeric network was formed. Mint extract was utilized for reducing agent of Ag^+ ion in the hydrogel network by a greener approach method.

3.1. Swelling of hydrogels

It has been noticed in the degree of swelling of pH sensitive hydrogels. These polymers identify in an incentive as a signal, magnitude and then alteration their chain conformation as a through response [1,9]. Fig. 1(a) has reflected the pH equilibrium swelling of hydrogels at room temperature in various pH media from acidic to alkaline (pH 3.0, pH 7.0 and pH 10.0).

The CFA biopolymeric hydrogels have shown a greater swelling at higher pH values, which perform like a polyelectrolyte. An anionic carboxylate groups has been protonated in low acidic medium, and the swelling of the CFA hydrogel network collapses. The weak poly acids bearing carboxylic acid group with pKa 5–6 shows the release of protons at neutral and high pH values. Fig. 1(b) has shown the swelling equilibrium of CFA hydrogels. When the CMC content is enhanced, swelling is increases and the composition of the fumaric acid is greatly affected by varying the swelling medium of pH. It has been concluded that the amount of CMC increased, swelling equilibrium of hydrogels has been improved, because of rise of ionizable functionalities (OH, $CONH_2$, COOH) and it is caused by the hydrodynamic free volume with solvent molecules [1,6,52]. Similarly, the best swollen hydrogels were chosen for the making of CFA (90:10) hydrogels. Fig. 1(c) indicating the better swelling profile of CFA (90:10) hydrogel. The CFA (90:10) hydrogel showed a lower swelling rate compared to all nanocomposite hydrogels in Fig. 1(d). This is due to maximum cavities and holes having been

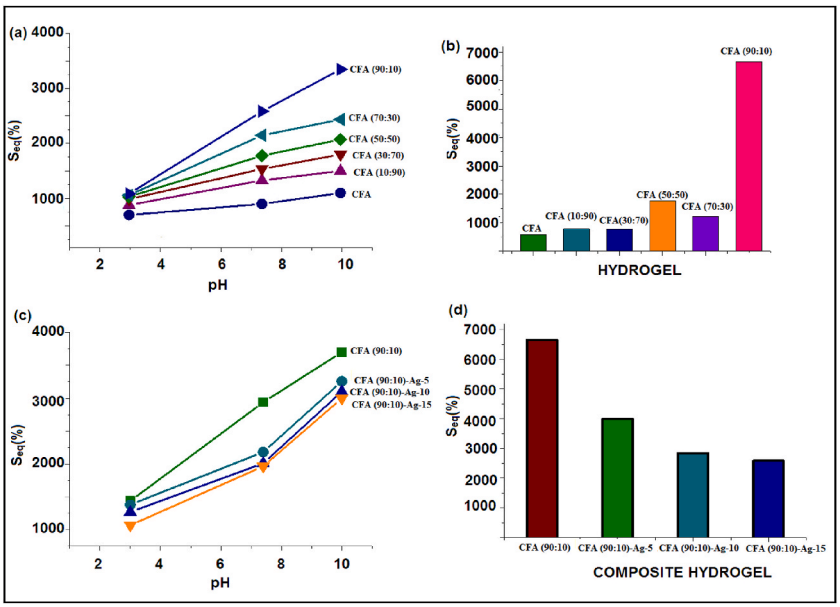

Fig. 1. (a) Swelling equilibrium of CFA hydrogels at various pH media (b) Swelling equilibrium of CFA hydrogels in distilled water (c) Swelling equilibrium of CFA-Ag nanocomposite hydrogels at various pH media (d) Swelling equilibrium of CFA-Ag nanocomposite hydrogels in distilled water.

occupied and the shrink of the hydrogel network [53]. For all these formulations, the arrangement of swelling capacity of parent hydrogels was estimated more than AgNPs incorporating nanocomposite hydrogels. This is due to reduction of Ag^{+} to Ag^{0} nanoparticles by the effect of addition of mint leaf extract, which might be diminish the complete porosity of hydrogels. Therefore, less intake of water has been observed.

3.2. FT-IR spectral studies

FT-IR spectra of NaCMC polyol, vinyl monomers (AAm and FA), and CFA biopolymeric hydrogels have been compared in Fig. 2(a). The spectra of NaCMC have noticed intense peaks at 800 and 1200 cm^{-1} exhibits to C–O, C–H stretching, CO and C–*O*–C flexible of a glycosidic structure of a polyol network. A wide absorption peak has been noticed at 3300-3500 cm^{-1} which is related to stretching frequency of –OH. The C–H stretching vibration has been recorded at 2940 cm^{-1}. A solid absorption peak has been noticed at 1626 and 1409 cm^{-1} because of asymmetric and symmetric stretching of COO-group, correspondingly. The peak at 1029.86 was attributed to –CH-*O*–CH_2– stretching frequency [54]. Other bands at 2440 and 1029 cm^{-1} corresponds to C–H stretching and CH_2 bending vibration respectively. The incorporation of AgNPs into hydrogel networks and intensity of bands has been changed in nanocomposite hydrogels [35] and the above statement well sustained the development and presence of AgNPs with in the hydrogel network [55].

Fig. 2(b) represents the FT-IR spectra of CFA (90:10)-Ag-5, CFA (90:10)-Ag-10, CFA (90:10)-Ag-20 nanocomposite hydrogels CFA (90:10)-Ag-5, CFA (90:10)-Ag-10, CFA (90:10)-Ag-20 nanocomposite hydrogels and CFA hydrogel has been exhibited a broad band at 3423 cm^{-1}, this is because of –OH stretching of –COOH and –NH stretching of an amide group and two peaks have looked and to have combined. The amide has shown a lesser carbonyl frequency than –COOH [56]. The sharp absorption band appeared at 1667 cm^{-1} in vinyl monomers viz., AAm, FA. The amide carbonyl group has shown a sharp absorption peak at 1600 cm^{-1}. The peak at 1425 cm^{-1} corresponds to the presence of COO- stretching frequency. The –NH stretching vibration of AAm has been observed at 3393 cm^{-1}. The disappearance of sharp peaks of C═C at 1667 cm-1 has shown the formation of hydrogels, which strongly supports the participation of monomers in free radical polymerization. Further, a broad band has been detected due to the presence of overlapped amide carbonyl and acid carbonyl at 1640 cm^{-1}. In addition, hydrogen bonded –NH and –OH broadened the peak to the range of 3300–3400 cm^{-1}. The formation and development of hydrogels has been revealed with the help of vanishment of characteristics peaks.

3.3. XRD analysis of hydrogels and their composites

X-ray diffraction (XRD) pattern is a versatile practice to detect the crystallinity of silver containing samples. Fig. 2(c) has shown the XRD arrangements of CFA hydrogel and its CFA (90:10)-Ag-5 and CFA (90:10)-Ag-20 nanocomposites hydrogels of two different concentrations (5 mM, 20 mM). The distinctive peaks have been observed and the parent CFA hydrogel has not been revealed every sharp peak in the XRD, which supports the amorphous nature of biopolymeric hydrogels. The CFA (10:90) nanocomposite hydrogels, sharp points were noticed at $2\theta = 27.00$, 32.00, and 46.00, which is verified by (111), (200), (220) and (311) reflections, because of the development of AgNPs within hydrogel. The diffraction peaks of CFA (90:10) for the AgNPs appearing at the 2θ value of 28, 33, 39, 47° were ascribed to (111), (200), (220), and (311) planes of face-centered cubic (FCC) of silver [57]. These obtained results have

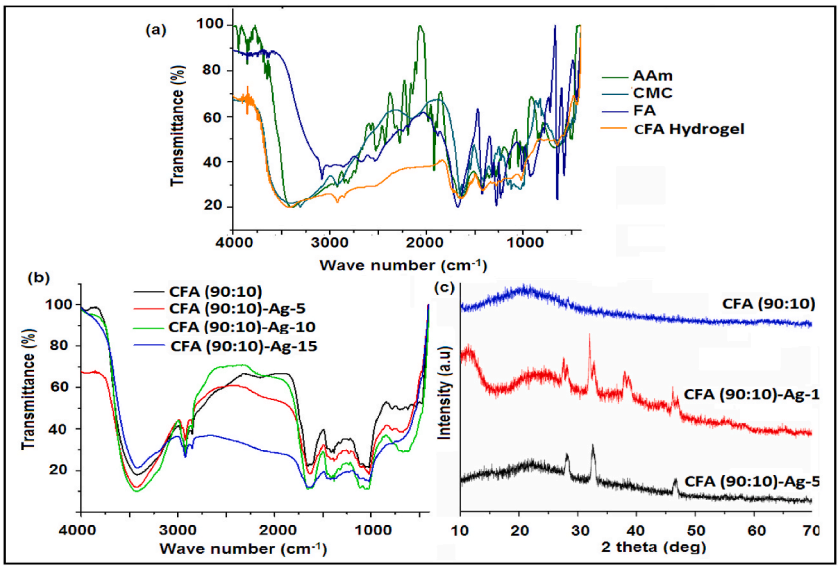

Fig. 2. (a) FT-IR spectra of CFA hydrogel, CMC polyol, FA and AAm monomers (b) FT-IR spectra of CFA (90:10)-Ag-5, CFA (90:10)-Ag-10, CFA (90:10)-Ag-20 nanocomposite hydrogels and CFA hydrogel (c) XRD pattern of CFA (90:10)-Ag-5 and CFA (90:10)-Ag-20 nanocomposite hydrogels and CFA hydrogel.

confirmed the formation of AgNPs inside the nanocomposites hydrogels. Thus, FTIR studies are attested by XRD analysis in the presence of AgNPs in nanocomposites.

3.4. Thermal analysis of hydrogels and their composites

3.4.1. Thermogravimetric analysis (TGA)

Two different hydrogels TGA curves were presented in Fig. 3(a). The two stages of degradation have been observed in NaCMC. The first stage has shown weight loss of around 10 % at 46–190 °C and the main weight loss of nearly 40 % happens at 240–300 °C [31]. The CFA (10:90) and CFA (90:10) hydrogel correspond to three stages of decomposition. In CFA (10:90) hydrogel, the initial stage weight loss was observed up to 220 °C and it is related with 13 % of moisture loss. Second stage weight loss 51 % at 220–475 °C corresponds to the degradation of NaCMC and pendant functionalities, decarboxylation, polyol and pendant acid group from 220 °C to 475 °C. Akar et al. also deal with the second stage degradation of NaCMC hydrogels started from 220 °C and attains maximum at 285 °C [30]. The third stage decomposition occurs at 475–785 °C, which corresponds to weight loss of 13.3 %. This is due to the carbonization and depolymerization of the main chain of polymeric hydrogels. Fig. 3(a) depicts the thermogram of CFA (90:10) hydrogels of three stages of decomposition. The initial thermal stability of CFA (10:90) hydrogel is higher than that of CFA (90:10). The thermal stability of hydrogels has been decided by an increasing composition of CMC from CFA (10:90) to CFA (90:10) and decreasing portion AAm.

The retaining capacity at 800 °C for CFA (10:90), CFA (90:10) hydrogels were found to be 21.10 and 25.42 %, and which is supporting that CFA (90:10) hydrogels is more stable than NaCMC and CFA (10:90) hydrogels. The enhanced thermal stability and rigid structure of the polymer of hydrogels might be due to the presence of MBA cross linker in the polymeric hydrogel network. Decreasing order of thermal stability as follows is CFA (90:10) > CFA (10:90>NaCMC. The nanocomposite hydrogels have noticed higher thermal stability than their respective hydrogels. The interaction of AgNps has encouraged the reduction of mobility of polymeric network chains and this leads to enhanced thermal stability. Fig. 3(a) has shown an interaction of AgNps within the hydrogels via acidic (COOH), hydroxyl (OH) and amide ($CONH_2$) groups, which is well supported by the results of FTIR spectrum analysis. The decomposition has been carried out at high temperature because of the interaction between the polymeric network and AgNps [58]. The obtained results revealed the synthesis of nanocomposite hydrogels has showed greater thermal stability than the parent hydrogels. This kind of nanocomposite hydrogel has exposed a potential application in many industrial applications.

3.4.2. Differential scanning calorimetry (DSC)

DSC curves of CFA (10:90) and CFA (90:10) hydrogels are represented in Fig. 3(b). A broad endotherm peak has been observed at 100–160 °C, which might be attributed for an evaporation of intake of water molecules. Two exothermic peaks were observed at 233.2 °C and 327.8 °C and two endothermic peaks were observed at 276.4 and 362.1 °C, which strongly supported the breakage of the CFA (10:90) polymeric hydrogel chain and carbonization of the hydrogel network. In addition, the CFA (90:10)-Ag-5 nanocomposite hydrogel has shown greater thermal stability than the CFA (10:90)-Ag-1. An extensive endotherm peak has been observed at 200–210 °C, due to ascribed to the evaporation of condensed water molecules. Similarly, for CFA (90:10) hydrogel, three endothermic peaks were observed at 100, 222.6, 352 °C and two exothermic peaks at 300 and 400 °C supported the thermal stability of hydrogels. This result has implied the successful crosslinking of CMC hydrogels with MBA. One exothermic peak has been observed at 320 °C, which toughly sustained the breakage of the CFA (10:90)-Ag-1 nanocomposite hydrogel. Similarly, For CFA (90:10)-Ag-5 nanocomposite hydrogel, one endothermic peak has been noticed at 220 °C and one exothermic peak at 350 °C maintained, which indicate the thermal stability nature of nanocomposite hydrogel. It is because of assimilation of more quantity of AgNPs inside the hydrogel network [59].

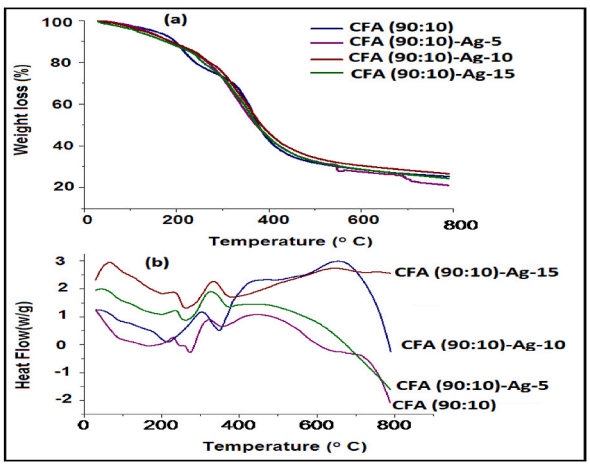

Fig. 3. Comparative thermogram TGA of CFA (10:90), CFA (90:10) hydrogels 3(a) and CFA (10:90)-Ag-1, CFA (90:10)-Ag-5 nanocomposite hydrogel 3(b).

3.5. Morphology studies: SEM and TEM analysis

3.5.1. SEM analysis of nanocomposite hydrogels

The SEM method is useful to reveal the structure of nanocomposite hydrogels [60]. Fig. 4(a-b) has shown SEM photographs of dried CFA hydrogel. The exterior morphology of the CFA hydrogel has been observed as an extremely rough and porous nature. CFA has also noticed a cohesive and dense structure because there are smooth and silky cavities on the surface. The presence of the rough and porous nature of the hydrogel network has been encouraged by swelling behaviour at various pH-media. The connectivity of apertures shows a vital role in speed of hydrogel swelling behaviour. The consistent holes or porous structure facilitates the dispersion of water molecules in and out over the hydrogel network [59].

3.5.2. TEM analysis of nanocomposite hydrogels

TEM studies have confirmed the fabrication of spherical AgNPs in CFA nanocomposite hydrogels as depicted in Fig. 4(c-d), which confirms the occurrence of AgNPs. A regular particle size of 15 nm has been formed which confirms the development of AgNPs within the nanocomposite hydrogels. The development of AgNPs CFA nanocomposite network is also supported by XRD analysis. The morphology of AgNPs in the range of 10–20 nm diameter [57]. Hence, the synthesized CFA (90:10)-Ag-5 and CFA (90:10)-Ag-20 nanocomposite hydrogels have been revealed in a circle-shaped nanostructure (50 nm).

3.6. Antibacterial activity of CFA nanocomposite hydrogels

Antimicrobial activity behaviour of CFA hydrogel and CFA (90:10)-Ag-20 nanocomposite hydrogels were carried out by disc diffusion technique using bacterial strains such as gram negative *E. coli* and gram positive *S. aureus* organism. In general, functional modified hydrogels have showed good antibacterial activity alongside usual bacteria, like *E. coli* and *S. aureus*. It has shown a vital role in medical fields such as wound dressings and tissue engineering etc [08]. $AgNP_S$ has also been noticed with better antibacterial power against pathogenic bacteria.

The synthesized CFA (90:10)-Ag-20 nanocomposite hydrogel has been proved to be an effective agent to resist microorganisms. The growing inhibitory effects have differed from one to another, which is noticed in Fig. 5(a–d). CFA (90:10)-Ag-20 has exhibited greater activity in the *E. coli* strain than the *S. aureus,* whereas CFA (90:10) possesses low biological activity. This is due to the incorporation of Ag^0 nanoparticles within the hydrogel network [61]. The AgNPs were able to stick on the bacteria cell wall, which penetrate over the cell membrane to kill microorganisms promptly. The silver cations have shown to have excellent antibacterial activity [62]. The minimum inhibitory concentrations (MIC) are the lowest concentrations (200 μg/mL) at which a compound can inhibit bacterium growth or kill more than 80 % of the added bacteria respectively. The CFA (90:10)-Ag-20 has been noticed. An effective antibacterial concentration is 20 μg/ml, which is comparatively less than ciprofloxacin 20 μg/ml. However, a similar effect has been observed in the bactericidal concentration of $AgNO_3$ and CFA (90:10). Therefore, the prepared CFA (90:10)-Ag-20 nanocomposite hydrogels and CFA (90:10) hydrogel have shown admirable antibacterial behaviour [63].

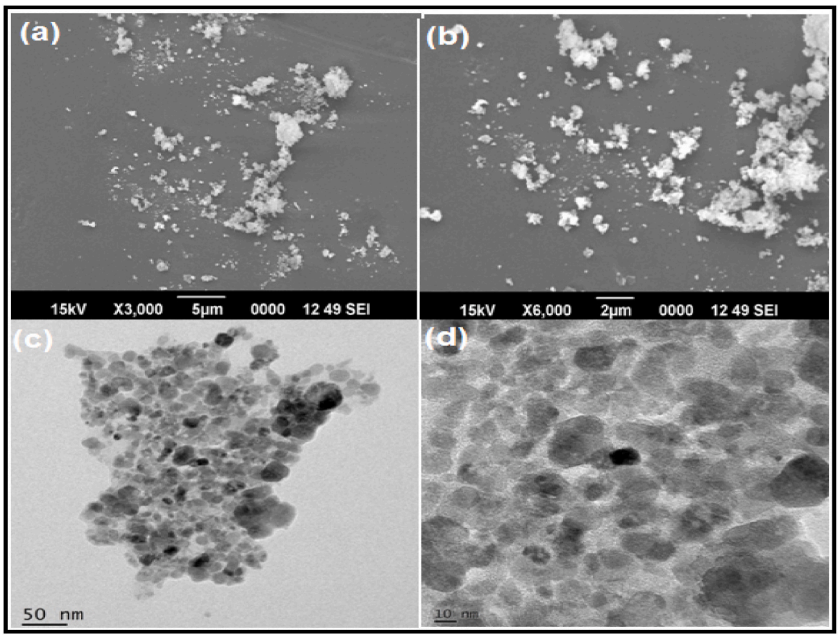

Fig. 4. (a–b) SEM images of CFA biopolymeric hydrogels, (c–d) TEM images of CFA (90:10)-Ag-5 and CFA (90:10)-Ag-20 nanocomposite hydrogels.

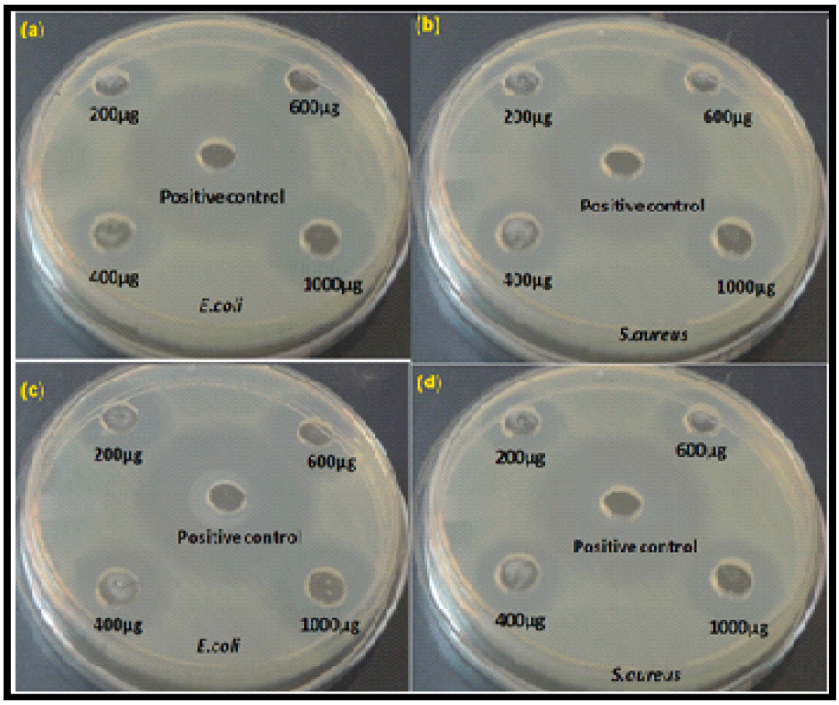

Fig. 5. (a–b): antibacterial activity of CFA (90:10)-Ag-20 nanocomposite hydrogels (c, d) antibacterial activity of CFA (90:10) bio-polymeric hydrogels.

4. Conclusions

In the present investigation, NaCMC polyol-based CFA hydrogels and their nanocomposite hydrogels have been fabricated through greener perspective method. A natural mint leaf extract is used as a reducing agent to avoid the effects of hazards and toxic chemicals. It exhibited pronounced swelling properties in water and different buffer medium from pH 3.0 to pH 10.0. Further, FTIR and XRD analysis confirms the formation of compounds and crystallinity of incorporation of AgNPs within hydrogel network with FCC crystal structure. Exploration of the SEM photographs has revealed that the AgNPs were homogeneously dispersed throughout the CFA hydrogel network. The agglomeration of AgNPs has been observed by TEM analysis in the range of 10–15 nm, which confirmed the nanocomposites' development as spherical in shape. Sustained antibacterial activity has been evaluated by *E. coli* (gram positive) and *S. aureus* (gram negative), which showed excellent antibacterial efficiency. Hence, the fabricated CFA hydrogels and nanocomposites may be employed for potential candidates for biomedical and environmental applications.

Ethical approval

Not applicable.

Informed consent

Not applicable.

Research involving human and animal participation

Not applicable.

CRediT authorship contribution statement

Shanmugavel Sudarsan: Conceptualization, Data curation, Formal analysis, Funding acquisition, Investigation, Methodology, Resources, Software, Validation, Visualization, Writing – original draft, Writing – review & editing. **Evgeny Trofimov:** Conceptualization, Data curation, Formal analysis, Funding acquisition, Investigation, Methodology, Resources, Software, Validation, Visualization, Writing – original draft, Writing – review & editing. **D.S. Franklin:** Conceptualization, Data curation, Formal analysis, Funding acquisition, Investigation, Methodology, Resources, Software, Validation, Visualization, Writing – original draft, Writing – review & editing. **Selvam Mullai Venthan:** Conceptualization, Data curation, Formal analysis, Investigation, Methodology, Validation,

Visualization, Writing – original draft, Writing – review & editing. **Selvam Guhanathan:** Conceptualization, Data curation, Formal analysis, Investigation, Methodology, Resources, Software, Validation, Visualization, Writing – original draft, Writing – review & editing. **Sanjay Mavinkere Rangappa:** Conceptualization, Data curation, Formal analysis, Investigation, Methodology, Resources, Software, Validation, Visualization, Writing – original draft, Writing – review & editing. **Suchart Siengchin:** Conceptualization, Data curation, Formal analysis, Investigation, Methodology, Resources, Software, Validation, Visualization, Writing – original draft, Writing – review & editing.

Declaration of competing interest

The authors declare that they have no known competing financial interests or personal relationships that could have appeared to influence the work reported in this paper.

References

[1] D.S. Franklin, Selvam Guhanathan, Influence of chain length of diol on the swelling behavior of citric acid based pH sensitive polymeric hydrogels: a green approach, J. Appl. Polym. Sci. 135 (2015) 5.
[2] X. Liu, J. Liu, S. Lin, X. Zhao, Hydrogel machines, Mater. Today 36 (2020) 102–124.
[3] X. Xu, V.V. Jerca, R. Hoogenboom, Bioinspired double network hydrogels: from covalent double network hydrogels via hybrid double network hydrogels to physical double network hydrogels, Mater. Horiz. 8 (2020) 1173–1188.
[4] S. Sudarsan, D.S. Franklin, M. Sakthivel, S. Guhanathan, Non-toxic, antibacterial, biodegradable hydrogels with pH-stimuli sensitivity: investigation of swelling parameters, Carbohydr. Polym. 148 (2016) 206–215.
[5] K. Varaprasad, K. Vimala, S. Ravindra, N.N. Reddy, K.M. Raju, Development of sodium carboxymethyl cellulose-based poly (acrylamide-co-2acrylamido-2-methyl-1-propane sulfonic acid) hydrogels for in vitro drug release studies of ranitidine hydrochloride an anti-ulcer drug, Polym.-Plast. Technol. Eng. 50 (12) (2011) 1199–1207.
[6] S. Sudarsan, M.S. Selvi, G. Chitra, S. Sakthivel, D.S. Franklin, S. Guhanathan, Nontoxic pH-sensitive silver nanocomposite hydrogels for potential wound healing applications, Polymer-Plastics Technology and Materials 60 (1) (2021) 84–104.
[7] G. Kougkolos, M. Golzio, L. Laudebat, Z. Valdez-Nava, E. Flahaut, Hydrogels with electrically conductive nanomaterials for biomedical applications, J. Mater. Chem. B 11 (10) (2023) 2036–2062.
[8] S.J. Jhaveri, M.R. Hynd, N. Dowell-Mesfin, J.N. Turner, W. Shain, C.K. Ober, Release of nerve growth factor from HEMA hydrogel-coated substrates and its effect on the differentiation of neural cells, Biomacromolecules 10 (1) (2009) 174–183.
[9] D. Şolpan, S. Duran, M. Torun, Removal of cationic dyes by poly (acrylamide-co-acrylic acid) hydrogels in aqueous solutions, Radiat. Phys. Chem. 77 (4) (2008) 447–452.
[10] S. Sant, S.L. Tao, O.Z. Fisher, Q. Xu, N.A. Peppas, A. Khademhosseini, Microfabrication technologies for oral drug delivery, Adv. Drug Deliv. Rev. 64 (6) (2012) 496–507.
[11] H. Mittal, R. Jindal, B.S. Kaith, A. Maity, S.S. Ray, Flocculation and adsorption properties of biodegradable gum-ghatti-grafted poly (acrylamide-co-methacrylic acid) hydrogels, Carbohydr. Polym. 115 (2015) 617–628.
[12] B. Manjula, K. Varaprasad, R. Sadiku, K. Ramam, G.V.S. Reddy, K.M. Raju, Development of microbial resistant thermosensitive Ag nanocomposite (gelatin) hydrogels via green process, J. Biomed. Mater. Res. 102 (4) (2014) 928–934.
[13] S. Sudarsan, D.S. Franklin, M. Sakthivel, G. Chitra, T.B. Sridharan, Ecofriendly pH-tunable hydrogels for removal of perilous thiazine dye,, J. Polym. Environ. 26 (9) (2018) 3773–3784.
[14] R. K. Wanchoo Thakur, P. Singh, Hydrogels of poly(acrylamide-co-acrylic acid): in-vitro study on release of gentamicin sulfate, Chem. Biochem. Eng. Q. 25 (4) (2011) 471–482.
[15] S.R. Van Tomme, G. Storm, W.E. Hennink, In situ gelling hydrogels for pharmaceutical and biomedical applications, Int. J. Pharm. 355 (1–2) (2008) 1–18.
[16] M. Sakthivel, D.S. Franklin, S. Sudarsan, G. Chitra, S. Guhanathan, Investigation on Au-nano incorporated pH-sensitive (itaconic acid/acrylic acid/triethylene glycol) based polymeric biocompatible hydrogels, Mater. Sci. Eng. C 75 (2017) 517–523.
[17] J.F. Gohy, B.G. Lohmeijer, S.K. Varshney, B. Décamps, E. Leroy, S. Boileau, U.S. Schubert, Stimuli-responsive aqueous micelles from an ABC metallo-supramolecular triblock copolymer, Macromolecules 35 (26) (2002) 9748–9755.
[18] D.C. Lin, B. Yurke, N.A. Langrana, Inducing reversible stiffness changes in DNA-crosslinked gels, J. Mater. Res. 20 (6) (2005) 1456–1464.
[19] B. Singh, R. Bala, Polysaccharide based hydrogels as controlled drug delivery system for GIT cancer, Int. J. Biol. Macromol. 65 (2014) 524–533.
[20] M. Pourmadadi, E. Rahmani, A. Shamsabadipour, A. Samadi, J. Esmaeili, R. Arshad, S. Pandey, Novel carboxymethyl cellulose based nanocomposite: a promising biomaterial for biomedical applications, Process Biochem. (2023).
[21] M. Mahdi Eshaghi, M. Pourmadadi, A. Rahdar, A.M. Díez-Pascual, Novel carboxymethyl cellulose-based hydrogel with core–shell Fe3O4@ SiO2 nanoparticles for quercetin delivery, Materials 15 (24) (2022) 8711.
[22] D.H.K. Reddy, S.M. Lee, Application of magnetic chitosan composites for the removal of toxic metal and dyes from aqueous solutions, Adv. Colloid Interface Sci. 201 (2013) 68–93.
[23] Y. Li, X. Hou, Y. Pan, L. Wang, H. Xiao, Redox-responsive carboxymethyl cellulose hydrogel for adsorption and controlled release of dye, Eur. Polym. J. 123 (2020), 109447.
[24] W. Chen, Y. Bu, D. Li, C. Liu, G. Chen, X. Wan, N. Li, High-strength, tough, and self-healing hydrogel based on carboxymethyl cellulose, Cellulose 27 (2020) 853–865.
[25] Y. Wang, X. Shi, W. Wang, A. Wang, Synthesis, characterization, and swelling behaviors of a pH-responsive CMC-g-poly (AA-co-AMPS) superabsorbent hydrogel, Turk. J. Chem. 37 (1) (2013) 149–159.
[26] G.O. Akalin, Alginate/carboxymethylcellulose-based hydrogels as pH-sensitive drug delivery systems: facile production with enhanced degradation, thermal and mechanical properties, Iran. Polym. J. (Engl. Ed.) (2023) 1–20.
[27] G.O. Akalin, Mehlika Pulat, Preparaation and characterization of nanoporous sosium carboxymethyl cellulose hydrogel beads, J. Nanomater. (2018).
[28] S.M. Ibrahim, K.M. El Salmawi, A.H. Zahran, Synthesis of crosslinked superabsorbent carboxymethyl cellulose/acrylamide hydrogels through electron-beam irradiation, J. Appl. Polym. Sci. 104 (3) (2007) 2003–2008.
[29] H. Savaş, O. Güven, Investigation of active substance release from poly (ethylene oxide) hydrogels, Int. J. Pharm. 224 (1–2) (2001) 151–158.
[30] E. Akar, A. Altınışık, Y. Seki, Preparation of pH-and ionic-strength responsive biodegradable fumaric acid crosslinked carboxymethyl cellulose, Carbohydr. Polym. 90 (4) (2012) 1634–1641.
[31] S. Yang, S. Fu, H. Liu, Y. Zhou, X. Li, Hydrogel beads based on carboxymethyl cellulose for removal heavy metal ions, J. Appl. Polym. Sci. 119 (2) (2011) 1204–1210.
[32] M. Dilaver, K. Yurdakoc, Fumaric acid cross-linked carboxymethylcellulose/poly (vinyl alcohol) hydrogels, Polym. Bull. 73 (2016) 2661–2675.
[33] S.I. Basha, S. Ghosh, K. Vinothkumar, B. Ramesh, K.M. Mohan, E. Sukumar, Fumaric acid incorporated Ag/agar-agar hybrid hydrogel: a multifunctional avenue to tackle wound healing, Mater. Sci. Eng. C 111 (2020), 110743.

[34] T. Menegatti, P. Žnidaršič-Plazl, Copolymeric hydrogel-based immobilization of yeast cells for continuous biotransformation of fumaric acid in a microreactor, Micromachines 10 (12) (2019) 867.
[35] E. Bozaci, E. Akar, E. Ozdogan, A. Demir, A. Altinisik, Y. Seki, Application of carboxymethylcellulose hydrogel based silver nanocomposites on cotton fabrics for antibacterial property, Carbohydr. Polym. 134 (2015) 128–135.
[36] A. Ortega, S. Valencia, E. Rivera, T. Segura, G. Burillo, Reinforcement of acrylamide hydrogels with cellulose nanocrystals using gamma radiation for antibiotic drug delivery, Gels 9 (8) (2023) 602.
[37] S.M. Nasef, E.E. Khozemy, G.A. Mahmoud, pH-responsive chitosan/acrylamide/gold/nanocomposite supported with silver nanoparticles for controlled release of anticancer drug, Sci. Rep. 13 (1) (2023) 7818.
[38] F. Zhang, C. Gao, S.R. Zhai, Q.D. An, Nanosilver anchored alginate/poly (acrylic acid/acrylamide) double-network hydrogel composites for efficient catalytic degradation of organic dyes, Front. Chem. Sci. Eng. (2023) 1–13.
[39] N. Annabi, J.W. Nichol, X. Zhong, et al., Controlling the porosity and microarchitecture of hydrogels for tissue engineering, Tissue Eng. B Rev. 16 (4) (2010) 371–383.
[40] W.E. Hennink, C.F. van Nostrum, Novel crosslinking methods to design hydrogels, Adv. Drug Deliv. Rev. 64 (2012) 223–236.
[41] G.R. Bardajee, Z. Hooshyar, H. Rezanezhad, A novel and green biomaterial based silver nanocomposite hydrogel: synthesis, characterization and antibacterial effect, J. Inorg. Biochem. 117 (2012) 367–373.
[42] M. Yadollahi, S. Farhoudian, S. Barkhordari, I. Gholamali, H. Farhadnejad, H. Motasadizadeh, Facile synthesis of chitosan/ZnO bio-nanocomposite hydrogel beads as drug delivery systems, Int. J. Biol. Macromol. 82 (2016) 273–278.
[43] F. Karchoubi, R.A. Ghotli, H. Pahlevani, M.B. Salehi, New Insights into Nanocomposite Hydrogels; A Review on Recent Advances in Characteristics and Applications, Advanced Industrial and Engineering Polymer Research, 2023.
[44] E. Sulastri, R. Lesmana, M.S. Zubair, A.F.A. Mohammed, K.M. Elamin, N. Wathoni, Ulvan/Silver nanoparticle hydrogel films for burn wound dressing, Heliyon 9 (7) (2023).
[45] Y.M. Bayisa, M.S. Bultum, Extraction of oil from Maesa lanceolata seeds and evaluation of its antimicrobial activities, S. Afr. J. Chem. Eng. 40 (1) (2022) 126–133.
[46] Y.M. Bayisa, T.A. Bullo, K.B. Hundie, D.A. Akuma, D.G. Gizachew, M.S. Bultum, Ecofriendly green synthesis and characterization of silver zinc oxide nanocomposite using the aqueous leaf extract of Rumex Crispus: evaluation of its antimicrobial and antioxidant activity, Heliyon 9 (5) (2023).
[47] M.A. Rojas, J. Amalraj, L.S. Santos, Biopolymer-based composite hydrogels embedding small silver nanoparticles for advanced antimicrobial applications: experimental and theoretical insights, Polymers 15 (16) (2023) 3370.
[48] Y.P. Moreno Ruiz, L.A. de Almeida Campos, M.A. Alves Agreles, A. Galembeck, I. Macário Ferro Cavalcanti, Advanced hydrogels combined with silver and gold nanoparticles against antimicrobial resistance, Antibiotics 12 (1) (2023) 104.
[49] M. Mojally, E. Sharmin, N.A. Obaid, Y. Alhindi, A.N. Abdalla, Polyvinyl alcohol/corn starch/castor oil hydrogel films, loaded with silver nanoparticles biosynthesized in Mentha piperita leaves' extract, J. King Saud Univ. Sci. 34 (4) (2022), 101879.
[50] T. Jayaramudu, G.M. Raghavendra, K. Varaprasad, R. Sadiku, K.M. Raju, Development of novel biodegradable Au nanocomposite hydrogels based on wheat: for inactivation of bacteria, Carbohydr. Polym. 92 (2) (2013) 2193–2200.
[51] K. Pal, A.K. Banthia, D.K. Majumdar, Esterification of carboxymethyl cellulose with acrylic acid for targeted drug delivery system, Trends Biomater. Artif. Organs 19 (1) (2005) 12–14.
[52] V.K. Takur, M.K. Takur, Handbook of polymers for pharmaceutical technologies, Handbook of Polymers for Pharmaceutical Technologies 1 (2015) 1–529.
[53] M. Yadollahi, H. Namazi, M. Aghazadeh, Antibacterial carboxymethyl cellulose/Ag nanocomposite hydrogels cross-linked with layered double hydroxides, Int. J. Biol. Macromol. 79 (2015) 269–277.
[54] Y. Qiu, K. Park, Environment-sensitive hydrogels for drug delivery, Adv. Drug Deliv. Rev. 53 (3) (2001) 321–339.
[55] Y.M. Mohan, T. Premkumar, K. Lee, K.E. Geckeler, Fabrication of silver nanoparticles in hydrogel networks, Macromol. Rapid Commun. 27 (16) (2006) 1346–1354.
[56] S.K. Bajpai, S. Singh, Analysis of swelling behavior of poly (methacrylamide-co-methacrylic acid) hydrogels and effect of synthesis conditions on water uptake, React. Funct. Polym. 66 (4) (2006) 431–440.
[57] S. Bhowmick, V. Koul, Assessment of PVA/silver nanocomposite hydrogel patch as antimicrobial dressing scaffold: synthesis, characterization and biological evaluation, Mater. Sci. Eng. C 59 (2016) 109–119.
[58] G.R. Bardajee, S.S. Hosseini, S. Ghavami, Correction to: embedded of nanogel into multi-responsive hydrogel nanocomposite for anticancer drug delivery, J. Inorg. Organomet. Polym. Mater. 29 (6) (2019) 2291, 2291.
[59] A. Hebeish, S. Sharaf, Novel nanocomposite hydrogel for wound dressing and other medical applications, RSC Adv. 5 (125) (2015) 103036–103046.
[60] A. Chandra Babu, M.N. Prabhakar, A. Suresh Babu, B. Mallikarjuna, M.C.S. Subha, K. Chowdoji Rao, Development and characterization of semi-IPN silver nanocomposite hydrogels for antibacterial applications, Int. J. Carbohydr. Chem. 2013 (2013).
[61] T. Jayaramudu, K. Varaprasad, G.M. Raghavendra, E.R. Sadiku, K. Mohana Raju, J. Amalraj, Green synthesis of tea Ag nanocomposite hydrogels via mint leaf extraction for effective antibacterial activity, J. Biomater. Sci. Polym. Ed. 28 (14) (2017) 1588–1602.
[62] S. Elbasuney, Green synthesis of hydroxyapatite nanoparticles with controlled morphologies and surface properties toward biomedical applications, J. Inorg. Organomet. Polym. Mater. 30 (3) (2020) 899–906.
[63] C.S. Kim, B. Duncan, B. Creran, V.M. Rotello, Triggered nanoparticles as therapeutics, Nano Today 8 (4) (2013) 439–447.